THE JOURNAL OF COMPARATIVE NEUROLOGY 413:342–355 (1999)

Topographic Organization of Serotonergic Dorsal Raphe Neurons Projecting to the Superior Colliculus in the Mongolian Gerbil (*Meriones unguiculatus*)

SKIRMANTAS JANUŠONIS,[1]* KATHERINE V. FITE,[1] AND WARREN FOOTE,[2]
[1]Neuroscience and Behavior Program, University of Massachusetts, Amherst, Massachusetts 01003
[2]Massachusetts General Hospital, Boston, Massachusetts 02114

ABSTRACT

Recent evidence suggests that the dorsal raphe nucleus (DRN) of the brainstem is a collection of neuronal clusters having different neurochemical characteristics and efferent projection patterns. To gain further insight into the neuroanatomic organization of the DRN, neuronal populations projecting to the superior colliculus (SC) were mapped in a highly visual rodent, the Mongolian gerbil (*Meriones unguiculatus*). Retrograde tracers Fluoro-Gold (FG) or cholera toxin subunit-B (CTB) were injected into the superficial layers of the SC, and serotonin (5-hydroxytryptamine, 5-HT) -positive cells were identified by using immunocytochemistry in the FG-injected animals. Based on its projections to the SC, the DRN was divided into five rostrocaudal levels. In the rostral and middle levels of the DRN, virtually all FG-filled cells occurred in the lateral DRN, and 36–55% of 5-HT-immunoreactive (5-HT-ir) cells were also double-labeled with FG. Caudally, FG-filled cells occurred in the lateral, ventromedial, and interfascicular DRN; and 44, 12, and 31% of 5-HT-ir cells, respectively, were also FG-filled. The dorsomedial DRN contained only a small proportion of FG-filled cells at its most caudal level and was completely devoid of FG-filled cells more rostrally. The CTB-injected animals showed a similar distribution of retrogradely labeled cells in the DRN. Topographically, the dorsal tegmental nucleus and the laterodorsal tegmental nucleus appeared to be closely associated with 5-HT-ir cells in the caudal DRN. These results suggest that the lateral DRN and the ventromedial/interfascicular DRN may be anatomically, morphologically, and neurochemically unique subdivisions of the gerbil DRN. J. Comp. Neurol. 413:342–355, 1999.

Indexing terms: dorsal raphe nucleus; serotonin (5-HT); visual system; dorsal tegmental nucleus; laterodorsal tegmental nucleus; topography

The raphe nuclei of the brainstem contain most of the serotonin (5-hydroxytryptamine, 5-HT) -producing neurons in the brain and are subdivided into superior and inferior groups. The inferior nuclei send descending projections to the brainstem, whereas the four superior, mesencephalic nuclei (dorsal raphe nucleus, DRN; median raphe nucleus, MRN; caudal linear nucleus, CLN; and the B9 group) project to mesencephalic, diencephalic, and telencephalic targets (Vertes, 1991; Jacobs and Azmitia, 1992; Vertes et al., 1999). The raphe nuclei are involved in the regulation, modulation, or both, of a broad range of systems, including sensory and motor functions, arousal and the sleep-wake cycle, and cognitive and affective behaviors (Van Bockstaele et al., 1993; Jacobs and Fornal, 1993; Shiromani and Schwartz, 1995; Cassel and Jeltsch, 1995; Montgomery, 1995; Harvey, 1996).

Several lines of evidence in different species suggest that the mesencephalic raphe system may be topographically organized, such that different target nuclei are

Grant sponsor: Whitehall Foundation; Grant sponsor: UMass-Baystate Collaborative Biomedical Research Program.

*Correspondence to: Skirmantas Janušonis, Neuroscience and Behavior Program, Tobin Hall, University of Massachusetts, Amherst, MA 01003. E-mail: janusonis@cas.umass.edu

Received 1 January 1999; Revised 14 May 1999; Accepted 30 June 1999

innervated by anatomically distinct subpopulations of raphe neurons. In rats, neurons projecting to the caudate-putamen and substantia nigra are located in the rostral portion of the DRN, whereas neurons projecting to the hippocampus and locus coeruleus are more caudal (Imai et al., 1986). Neurons projecting to the medial prefrontal cortex are clustered in the medial DRN (Van Bockstaele et al., 1993). The anterior thalamic nucleus receives a serotonergic projection from the ventromedial and ventrolateral part of the ipsilateral DRN (Gonzalo-Ruiz et al., 1995), whereas the piriform cortex is innervated by neurons in the ventromedial DRN (Datiche et al., 1995). Rat raphe neurons innervating the ventricular system appear to be distributed in the intermediate dorsomedial DRN (Simpson et al., 1998).

Specific visual nuclei also receive differential projections from anatomically distinct neuronal subpopulations in the mesencephalic raphe system. In hamsters and rats, the MRN projects to the suprachiasmatic nucleus (Meyer-Bernstein and Morin, 1996; Moga and Moore, 1997; Leander et al., 1998), whereas in hamsters, the DRN sends axons to the intergeniculate leaflet (Meyer-Bernstein and Morin, 1996). The caudal DRN projects to the pineal gland in the golden hamster (Leander et al., 1998). In rats, neurons projecting to the visual cortex are clustered in the ventromedial portion of the rostral two-thirds of the DRN, between the medial longitudinal fasciculi (Waterhouse et al., 1993). Koh et al. (1991) obtained somewhat different results, with most of the neurons projecting to the visual cortex being localized in the midcaudal region of the DRN. If the tracer injection was restricted to the superficial and intermediate layers of the rat superior colliculus, retrogradely labeled serotonergic neurons occurred predominantly in the DRN (Beitz et al., 1986). Similar results have been obtained in the cat (Mize and Horner, 1989). In rats, injections into the superior colliculus and lateral geniculate nucleus (LGN) retrogradely labeled neurons in the ipsilateral lateral wings of the DRN (Villar et al., 1988; Waterhouse et al., 1993). Also, the same serotonergic neuron may send axonal branches both to the superior colliculus and to the lateral geniculate nucleus (Villar et al., 1988).

The data on the neurochemical identity of DRN neurons innervating different target nuclei are sparse and incomplete. Neurons in the DRN contain a large variety of neurotransmitters, some of which may be colocalized. Most DRN neurons produce 5-HT, and 5-HT–immunoreactive neurons are conventionally used to delineate the DRN itself. However, it is estimated that approximately 30% of the neurons in the cat DRN are not serotonergic (Wiklund et al., 1981). Neurons in the DRN may produce GABA (Stamp and Semba, 1995), glutamate (Clements and Grant, 1990), enkephalins (Leger et al., 1986), substance P (SP) (Chan-Palay et al., 1978), and other neurotransmitters and neuromodulators. It is likely that neuronal subpopulations revealed by tracing studies may contain a specific subset of these neurotransmitters. For example, squirrel-monkey DRN neurons have been shown to be segregated according to their neurotransmitter immunoreactivity (Charara and Parent, 1998). In rats, vasoactive intestinal polypeptide (VIP)–immunoreactive neurons are located in the dorsal part of the DRN (Petit et al., 1995). Approximately half of rat DRN neurons projecting to the visual cortex are serotonergic (Koh et al., 1991). According to Beitz et al. (1986), 65% of rat DRN neurons projecting to the superior colliculus are serotonergic, whereas, in the cat, they seem to be exclusively serotonergic (Mize and Horner, 1989).

To provide further insight into the organization of the DRN, the present study has focused on the anatomic localization of serotonergic DRN neurons projecting to the superior colliculus in the Mongolian gerbil. Unlike rats, gerbils are crepuscular/diurnal in their habits and have a well-developed visual system (Pietrewicz et al., 1982; Susic and Masirevic, 1986; Govardovskii et al., 1992). Also, a direct projection from the retina to the DRN has been described in gerbils (Fite et al., 1998), which is more extensive than has been previously reported in rats (Shen and Semba, 1994).

MATERIALS AND METHODS

Animals

Adult gerbils weighing 60–75 g were anesthetized with a mixture of ketamine (100 mg/kg) and xylazine (10 mg/kg). All experiments were approved by the Institutional Animal Care and Use Committee of the University of Massachusetts at Amherst in accordance with National Institutes of Health and United States Department of Agriculture guidelines.

Tracer injections

By using a 10 μl-Hamilton syringe, a 5% Fluoro-Gold (FG; Fluorochrome, Inc., Englewood, CO) solution in distilled water was pressure-injected stereotaxically into the superficial layers of both superior colliculi in three animals (0.4–0.5 μl on each side) and into the superficial layers of the right superior colliculus in one animal (0.5 μl). The stereotaxic coordinates were (with respect to the lambda point) 1.0 mm anterior, 1.0 mm lateral, and 3.0 mm below the dura. The needle was left in place for at least 10 minutes after the injection was complete. After injections, the skull was sealed with bone wax and the incision was closed with stainless steel wound clips.

In three additional animals, a solution of 2% cholera toxin subunit B (CTB low salt; List Biological Laboratories, Inc., Campbell, CA) dissolved in 2% dimethyl sulfoxide was injected bilaterally into the superficial layers of the superior colliculi (1.5 μl on each side). The CTB injections were performed in the same manner as the FG injections.

Histology and immunocytochemistry

After a 7- to 9-day survival period, both FG- and CTB-injected animals were deeply anesthetized with Nembutal. The exposed heart immediately was injected with 0.2 ml of heparin (5,000 USP U/ml), and the animal was perfused with saline followed by 400 ml of chilled 4% paraformaldehyde in 0.1 M phosphate buffer (PB, pH 7.2). The brains were removed, post-fixed in the same fixative overnight at 4°C, and transferred to 30% sucrose in PB. The following day, serial, coronal sections were cut on a freezing microtome at 40 μm thickness and were stored in cryoprotectant. The plane of sectioning was comparable to that shown in the Paxinos and Watson (1998) rat brain atlas.

CTB immunocytochemistry was performed by using a highly sensitive protocol (Angelucci et al., 1996). Free-floating sections were rinsed (four times, 5 minutes each) in 0.1 M phosphate buffered saline (PBS, pH 7.4); incu-

bated in 0.3% H_2O_2 in PBS for 20 minutes; rinsed in PBS (three times, 5 minutes each); incubated in 0.1 M glycine in PBS for 30 minutes; rinsed in PBS (three times, 5 minutes each); and incubated in 4.5% normal rabbit serum (NRS; Vector Laboratories, Burlingame, CA), 2.5% bovine serum albumin (BSA, Sigma), and 0.4% Triton X-100 (TX) in PBS overnight at 4°C. Sections were rinsed two times (5 minutes each) in PBS, and incubated in a goat anti-CTB antibody (1:4,000, List Biological Laboratories, Inc.) solution containing 2% NRS, 2.5% BSA, and 2% TX for 4 days at 4°C. Sections were rinsed four times (15 minutes each) in PBS; incubated in 2% NRS and 2.5% BSA in PBS for 10 minutes; incubated in biotinylated rabbit anti-goat antibody (Vector Laboratories), diluted 1:200 in 2% NRS, 2.5% BSA, and 1% TX in PBS for 1.5 hours; rinsed four times (15 minutes each) in PBS; incubated again in 2% NRS and 2.5% BSA in PBS for 10 minutes; incubated in a 1:100 avidin-biotin-peroxidase complex (ABC Elite, Vector Laboratories) solution in PBS for 1 hour; rinsed four times (15 minutes each) in PBS; rinsed two times (5 minutes each) in 0.05 Tris-buffer (TB, pH 7.4); incubated in 0.5% $CoCl_2$ in TB for 10 minutes; rinsed in TB for 1 minute; rinsed two times in PBS (5 minutes each); preincubated in 3,3′-diaminobenzidine (0.05%) in PBS for 5 minutes; and reacted (3 minutes) by adding 0.01% H_2O_2 to the 3,3′-diaminobenzidine solution. Sections then were rinsed five times (1 minute each) in PBS, mounted on chromium-subbed slides, allowed to air-dry, cleared with Hemo-De, and cover-slipped with Permount.

Brain sections from the FG-injected animals were processed for 5-HT immunoreactivity by using the described CTB protocol, which was modified as follows: the goat anti-CTB antibody was replaced with a rabbit anti-5-HT antibody (Protos Biotech, New York, NY; catalog no. NT102) at a dilution of 1:300; the rabbit anti-goat antibody was replaced with a TRITC-conjugated donkey anti-rabbit antibody (1:100, Jackson ImmunoResearch Laboratories, Inc., West Grove, PA); and the NRS was replaced with normal donkey serum (Jackson ImmunoResearch Laboratories, Inc.). After the incubation in the solution containing the TRITC-conjugated donkey anti-rabbit antibody, sections were rinsed four times in PBS (15 minutes each), mounted on chromium-subbed slides, allowed to air-dry in the dark, cleared in Hemo-De, and cover-slipped with Krystalon.

Tissue analysis

Sections labeled for both FG and 5-HT were analyzed by using a fluorescent Leica DMR microscope. Individual 5-HT–immunoreactive (5-HT-ir) and FG-filled and double-labeled cells were counted in every other section for all bilaterally injected gerbils. The percentages of double-labeled cells in different areas of the DRN were compared by using the paired t-test. Photographs of fluorescent sections were taken by using Kodak TMAX 3200 ASA film. Sections from CTB-injected gerbils were used to confirm the location and distribution of neurons within the DRN as revealed in the double-labeling experiments.

The nomenclature describing neuronal subpopulations in the DRN is still being developed in accordance with emerging neuroanatomic and neurochemical data, and different authors use slightly different terminology. The rat DRN has been recently subdivided into caudal, interfascicular, dorsal, ventral, and ventrolateral regions (Paxinos and Watson, 1998). In the present study, neuronal populations in the gerbil DRN were compared with similar populations as described in other species.

RESULTS

Injection sites

Dense FG deposits were seen in the superficial and intermediate layers throughout the rostrocaudal extent of the superior colliculi (SC), with necrotic areas around the injection sites located midway between the rostral and caudal poles (Fig. 1). These areas of bright FG fluorescence are generally considered to represent the effective injection site (Moga and Saper, 1994; Leak and Moore, 1997). The distribution of 5-HT-immunoreactive (5-HT-ir) fibers appeared somewhat more dense around the FG injection sites, especially near the necrotic areas. These fibers may be damaged or regenerating serotonergic axons (Haring, 1991; Chauvet et al., 1998).

The ventral lateral geniculate nucleus, the intergeniculate leaflet, the laterodorsal tegmental nucleus, and the locus coeruleus were retrogradely labeled in all animals; all of these nuclei are known to project to the SC (Cornwall et al., 1990; Waterhouse et al., 1993; Harrington, 1997). The zona incerta also was labeled in all animals, indicating that the effective injection site included the rostral pole of the superior colliculus as well (Jiang et al., 1997). Many FG-filled cells were observed in the inferior colliculus, but these were probably the result of retrograde labeling from the SC, which receives efferents from the external nucleus of the inferior colliculus (King et al., 1998). The ventral cochlear nucleus was not labeled.

Distribution of FG-labeled and 5-HT-ir cells in the DRN

In the DRN, retrogradely labeled 5-HT-ir cells were clustered into well-defined subpopulations. In coronal sections, the localization and appearance of these subpopulations tended to remain relatively constant through several rostrocaudal, serial sections before a new, topographically distinct configuration appeared. On the basis of the characteristic appearance of these subpopulations, the DRN was subdivided into five rostrocaudal levels (Fig. 2). The most rostral level has been designated as "Level 1" (DRN-L1) and the most caudal level as "Level 5" (DRN-L5). The proportions of double-labeled (5-HT-ir and FG-filled) cells in all DRN subpopulations of these five levels are summarized for three cases in Tables 1 and 2.

DRN rostrocaudal Level 1

The DRN rostrocaudal Level 1 (DRN-L1) represents the most rostral portion of the DRN (Figs. 2, 3A). At its most rostral end, sparsely distributed 5-HT-ir neurons occurred lateral to the midline. Moving caudally within Level 1, 5-HT-ir neurons gradually increased in number, and a medial 5-HT-ir population also emerged. Neurons in the lateral DRN generally showed higher 5-HT immunoreactivity than did neurons in the medial DRN and seemed to be segregated into dorsolateral and ventrolateral clusters (Fig. 3C). The dorsolateral cell populations were located ventral to the aqueduct, whereas the ventrolateral cell populations bordered the oculomotor nuclei (n. III).

All FG-filled cells were clustered in the dorsolateral and ventrolateral DRN (Fig. 3D). No retrogradely labeled cells were observed in the medial DRN at this level. Approximately 46% of 5-HT-ir cells in the dorsolateral DRN and

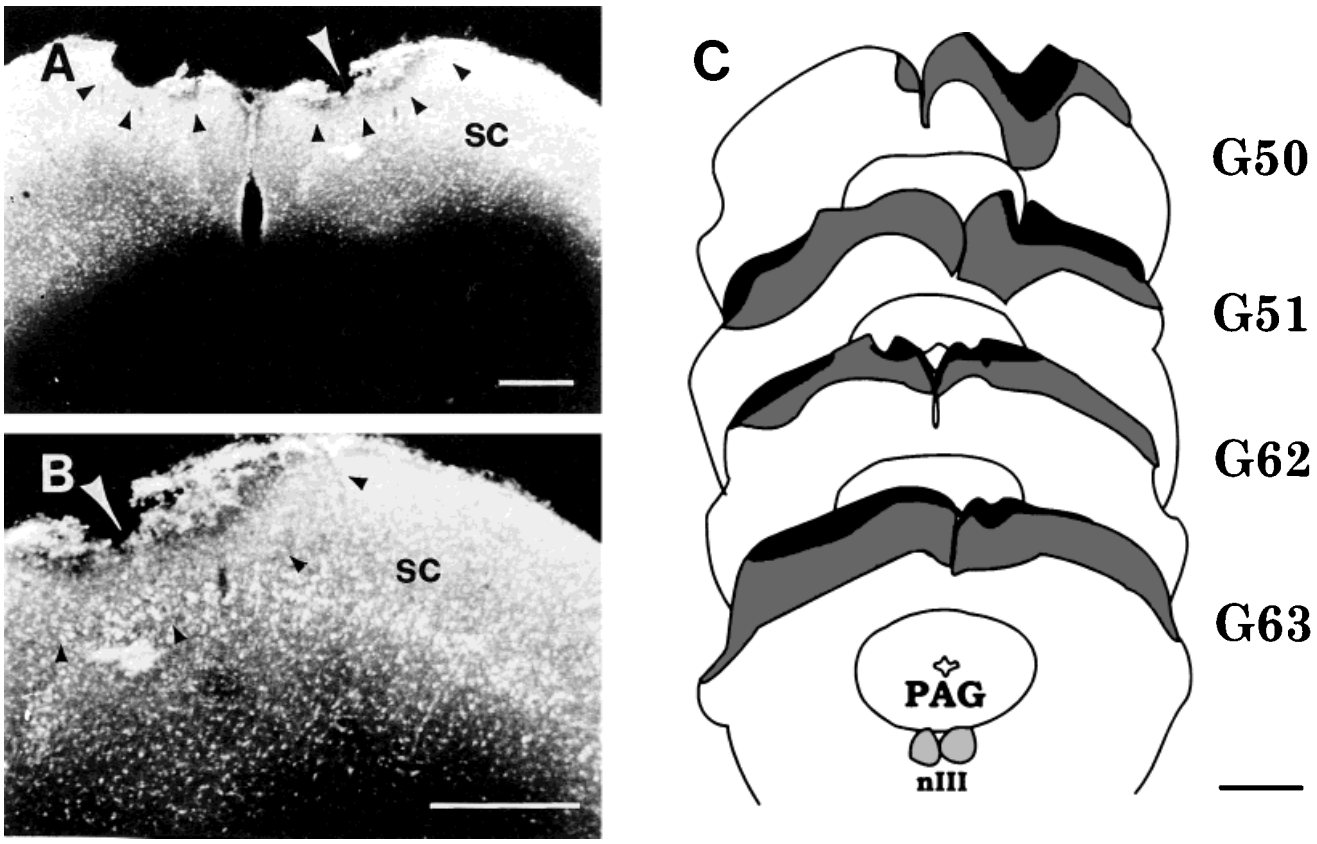

Fig. 1. Photomicrographs of Fluoro-Gold (FG) bilateral injection sites in the superficial layers of the superior colliculus (SC) in case G62. **A,B:** White arrowheads indicate a point of correspondence. Black arrowheads indicate the necrotic region. **C:** Schematic representation of FG injection sites in four cases (G50, G51, G62, G63). Necrotic areas around the injection sites are shown in black; regions with dense FG label are shown in gray. PAG, periaqueductal gray; nIII, oculomotor nucleus. Scale bar = 500 μm in A,B, 1,000 μm in C.

55% 5-HT-ir cells in the ventrolateral DRN were FG filled; this difference was not significant ($P > 0.10$). Approximately 35% of FG-filled cells in the dorsolateral DRN and 32% of FG-filled cells in the ventrolateral DRN were not 5-HT immunoreactive. Retrogradely labeled neurons also occurred in both lateral populations in CTB-injected gerbils, with virtually no CTB-filled cells in the medial DRN (Fig. 3B).

DRN rostrocaudal Level 2

At DRN rostrocaudal Level 2 (DRN-L2), the broad lateral wings of the DRN occurred dorsally, adjacent to the aqueduct (Figs. 2, 4A). The ventral portion of the DRN was located medially and bordered the oculomotor nuclei (n. III). At this level, all FG-filled cells were clustered in the lateral wings, and approximately 37% of all 5-HT-ir neurons in the lateral wings were also FG filled. Large, clearly multipolar, double-labeled cells were observed, some with a long process extending dorsally along the ependymal wall of the aqueduct (Fig. 4C,D). The medial portion of the DRN was devoid of FG-labeled cells. Approximately 46% of FG-filled cells in the lateral wings were not 5-HT immunoreactive. Virtually all CTB-filled cells also occurred in the lateral wings of the DRN (Fig. 4B).

DRN rostrocaudal Level 3

At DRN rostrocaudal Level 3 (DRN-L3), the DRN lateral wings were most extensive and lay roughly equidistant between the aqueduct and the medial longitudinal fasciculi (MLF) (Figs. 2, 5A). The lateral DRN and the medial DRN showed different intensities of 5-HT immunoreactivity: 5-HT-ir cells in the lateral wings were always more intensely fluorescent than 5-HT-ir cells in the medial DRN (Fig. 5B). Virtually all FG-filled cells occurred in the lateral wings (Fig. 5C). Some double-labeled (5-HT-ir and FG-filled) cells were observed dorsally, near the aqueduct, or ventrally, near the MLF, forming dorsal and ventral extensions of the lateral wings (Fig. 2, Level 3). Approximately 36% of all 5-HT-ir neurons in the lateral wings were also FG filled, and approximately 34% of FG-filled cells in these populations were not 5-HT immunoreactive. FG-filled cells were generally absent from the medial portion of the DRN. In the unilaterally injected case (G50), Level 3 was the only level at which an asymmetry was observed in the distribution of ipsilateral vs. contralateral FG-filled cells. Although both ipsilateral and contralateral cells formed well-defined clusters in the lateral DRN, more FG-filled cells occurred in the ipsilateral cluster. In CTB-injected gerbils, the densest clustering of CTB-labeled cells also occurred in the lateral wings, although occasional CTB-labeled cells were scattered in the medial DRN.

DRN rostrocaudal Level 4

DRN rostrocaudal Level 4 (DRN-L4) was easily recognized by intensely 5-HT-immunoreactive plexuses in the

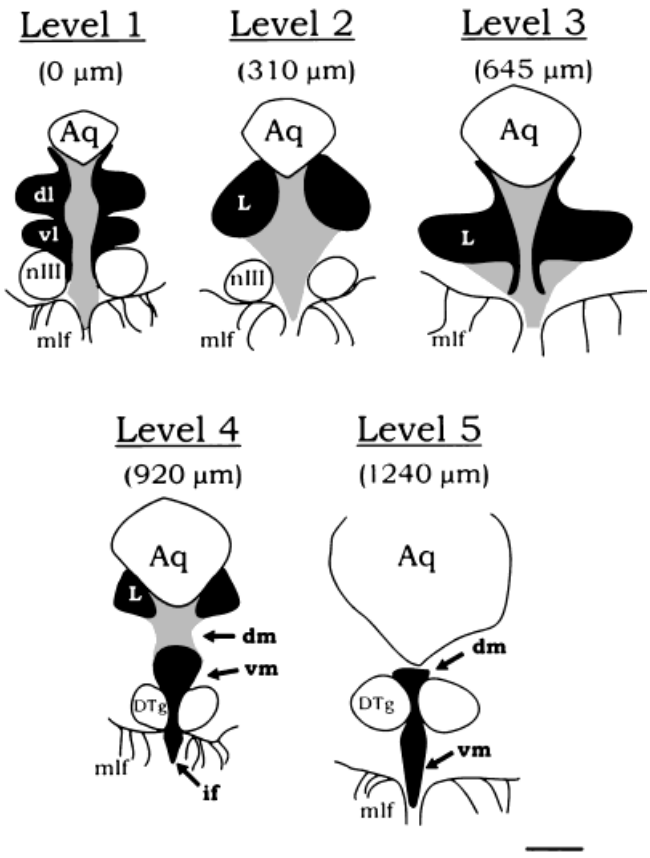

Fig. 2. Schematic representation of 5-HT-immunoreactive (5-HT-ir) and Fluoro-Gold (FG) retrogradely labeled cells at different coronal levels in the dorsal raphe nucleus (DRN) after a bilateral FG injection into the superior colliculus. Gray and black areas represent the distribution of 5-HT-ir cells, whereas black areas show the subpopulations of 5-HT-ir cells that are also labeled with FG. Individual subpopulations of DRN neurons are indicated as follows: dl, dorsolateral; vl, ventrolateral; L, lateral; dm, dorsomedial; vm, ventromedial; if, interfascicular. Numbers under each level indicate distance between successive coronal levels beginning with the most rostral Level 1 (0 μm). Aq, aqueduct; nIII, oculomotor nucleus; mlf, medial longitudinal fasciculus; DTg, dorsal tegmental nucleus. Scale bar = 300 μm.

TABLE 1. Double-Labeled Cells in Levels 1–3[1] (Cases G51, G62, G63)

	L (% ± SEM)		dl (% ± SEM)		vl (% ± SEM)	
Level	db/5-HT[2]	db/FG[3]	db/5HT	db/FG	db/5HT	db/FG
1			42 ± 5	58 ± 4	51 ± 6	67 ± 5
	—	—	46 ± 3	75 ± 3	56 ± 4	71 ± 6
			49 ± 5	62 ± 6	58 ± 4	67 ± 5
2	43 ± 5	29 ± 2				
	37 ± 5	66 ± 6	—	—	—	—
	33 ± 4	67 ± 5				
3	29 ± 4	50 ± 6				
	39 ± 5	80 ± 2	—	—	—	—
	41 ± 4	69 ± 5				

[1]Abbreviations: L, lateral dorsal raphe nucleus (DRN); dl, dorsolateral DRN; vl, ventrolateral DRN; 5-HT, 5-hydroxytryptamine; FG, Fluoro-Gold.
[2]Proportion of 5-HT-immunoreactive cells that were also FG filled.
[3]Proportion of FG-filled cells that were also 5-HT immunoreactive.

dorsal tegmental nuclei (DTg) that flanked the ventral portion of the DRN (Figs. 2, 6A,C). These 5-HT-ir plexuses proved to be an extremely useful landmark in defining the borders of different subpopulations of double-labeled cells in the caudal DRN. At the most rostral end of Level 4, these plexuses were located on both sides of the midline just above the MLF. More caudally, they were larger and oval-shaped, with 5-HT immunoreactivity gradually fading away at their lateral edges. Ventrally, these plexuses isolated a small interfascicular population of 5-HT-ir cells, 31% of which were also FG filled (Fig. 6B). The rest of the 5-HT-ir cells were located dorsal to the DTg plexuses and could be subdivided into several, clearly defined clusters. The area immediately dorsal to the DTg plexuses (ventromedial DRN) contained 5-HT-ir neurons that were also FG filled (12%). In contrast, the dorsomedial cluster located above the ventromedial cell population and below the aqueduct was completely devoid of FG-labeled cells (Fig. 6B). Interestingly, the density, size, and morphology of 5-HT-ir neurons in the dorsomedial DRN were comparable to those in the ventromedial DRN. The difference in the proportion of double-labeled cells in the ventromedial DRN vs. the interfascicular DRN was significant in one case (G51: $P < 0.02$) and approached significance in two other cases (G62 and G63: $P < 0.07$). In the ventromedial and interfascicular regions of the DRN, the proportions of FG-filled cells that were not 5-HT immunoreactive were 33% and 25%, respectively.

Immediately below the aqueduct, two populations of 5-HT-ir neurons were observed laterally on each side of the dorsomedial DRN (Fig. 2, Level 4). These populations did not appear to be simply a lateral extension of the dorsomedial population. Unlike the dorsomedial DRN, they contained a very high proportion of 5-HT-ir cells that were also FG filled (44%). Also, most of the cells in the lateral populations were multipolar and showed higher immunoreactivity than 5-HT-ir cells located medially. The most lateral edge of the lateral DRN seemed to be a transition zone between the DRN and the laterodorsal tegmental nucleus (LDTg). Many 5-HT-ir neurons were FG filled in this region and were intermingled with a population of smaller, FG-filled, non–5-HT-ir cells in the LDTg (Fig. 6A,B).

In CTB-injected gerbils, the dorsomedial population appeared to undergo a complex transition from Level 4 to Level 5. At the caudal end of Level 4, retrogradely labeled neurons in the dorsomedial DRN formed a ring-like configuration that was not visible in FG-injected gerbils (Fig. 7B).

DRN rostrocaudal Level 5

DRN rostrocaudal Level 5 (DRN-L5) lies at the most caudal pole of the DRN (Figs. 2, 7A). At this level, the DRN was defined by a median strip of 5-HT-ir cells that was flanked by two large (350 μm), oval-shaped, 5-HT-ir plexuses in the DTg (Fig. 7D). These plexuses were less intensely 5-HT immunoreactive than those in Level 4 and appeared to "squeeze" the DRN in the middle, dividing it into dorsomedial and ventromedial portions. The dorsomedial population lay immediately below the aqueduct, whereas the ventromedial population extended ventrally to the MLF. Although both populations contained FG-filled cells (Fig. 7E), most of them occurred in the ventromedial DRN. Only 3% of all 5-HT-ir cells in the dorsomedial DRN were also filled with FG, compared with approximately 28% of all 5-HT-ir cells in the ventromedial DRN that were also filled with FG. This difference was significant in all three bilaterally injected gerbils (G51: $P < 0.03$; G62 and G63: $P < 0.01$). Approximately 23% of FG-filled cells in the dorsomedial population and 33% of FG-filled cells in the ventromedial population were not 5-HT immunoreactive.

TABLE 2. Double-Labeled Cells in Levels 4 and 5[1] (Cases G51, G62, G63)

	dm (% ± SEM)		vm (% ± SEM)		if (% ± SEM)		L (% ± SEM)	
Level/Clusters	db/5HT	db/FG	db/5HT	db/FG	db/5HT	db/FG	db/5HT	db/FG
4	0 ± 0	—	12 ± 3	74 ± 11	39 ± 5	84 ± 6	41 ± 3	67 ± 17
	0 ± 0	—	12 ± 4	61 ± 7	25 ± 0	58 ± 7	39 ± 7	43 ± 12
	0 ± 0	—	11 ± 1	65 ± 8	28 ± 5	82 ± 12	52 ± 5	77 ± 23
5	3 ± 1	81 ± 11	45 ± 11	67 ± 7				
	4 ± 1	66 ± 12	19 ± 2	69 ± 9	—	—	—	—
	3 ± 1	83 ± 11	20 ± 4	66 ± 14				

[1]Abbreviations: dm, dorsomedial dorsal raphe nucleus (DRN); vm, ventromedial DRN; if, interfascicular DRN; L, lateral DRN. For other abbreviations, see Table 1.

Compared with cases with FG injections in the SC, CTB-injected gerbils contained more retrogradely labeled cells in the dorsomedial cluster (Fig. 7C). In the absence of 5-HT label, it was difficult to determine whether this cluster occupied the whole dorsomedial DRN or just its medial portion.

DISCUSSION

Retrogradely labeled neurons

The present study has revealed a more conspicuous segregation of SC-projecting neurons in the gerbil DRN than has been previously shown in the rat. In the rat, retrogradely labeled cells occurred close to the midline beneath the cerebral aqueduct and in the lateral wings of the DRN; also, they were more numerous in the middle one-third of the DRN (Waterhouse et al., 1993). In the gerbil DRN, the laterality of retrogradely labeled cells depended on the particular coronal level. Rostrally (Levels 1–3), nearly all retrogradely labeled cells occurred in the lateral DRN and very few labeled cells were close to the midline. More caudally (Levels 4 and 5), many retrogradely labeled cells occurred in the medial DRN, but their number varied as a function of the dorsoventral subdivision of the DRN (see Table 2). Retrogradely filled cells appeared to form well-defined clusters, and both the location and appearance of these clusters were the same in all gerbils, even though two different tracers were used and the SC injection sites varied slightly. Some of these differences between the rat and the gerbil could be due, in part, to methodologic differences. For example, in the present study, FG and CTB were injected bilaterally into the SC in gerbils; whereas, in rats, Waterhouse et al. (1993) made unilateral wheat germ agglutinin-horseradish peroxidase injections into the SC. Also, in the present study, the DRN was specifically defined by the distribution of 5-HT-ir cells. This mapping of 5-HT-ir cells was particularly important in delineating the lateral boundaries of the DRN, because some SC-projecting neurons also occurred in other nuclei adjacent to the DRN (e.g., LDTg, Fig. 6).

Although the proportion of 5-HT-ir DRN neurons that were projecting to the SC varied from one neuronal population to another (0–55%), the proportion of SC-projecting neurons that were not 5-HT immunoreactive showed much less variability (23–46%). These numbers are consistent with the proportion of nonserotonergic DRN neurons (35%) that project to the SC in the rat (Beitz et al., 1986). In contrast, almost all SC-projecting neurons in the cat DRN appear to be serotonergic (Mize and Horner, 1989).

It should be noted that the actual numbers of SC-projecting 5-HT-ir neurons in gerbils may be higher than detected in these double-labeling experiments. Although the numbers of FG- and CTB-labeled cells were similar throughout the DRN, more retrogradely labeled neurons were observed in the caudal dorsomedial DRN in CTB-injected cases. In addition, CTB-labeling revealed a ring-like cluster of retrogradely labeled neurons in this area, that was not detected in FG-injected animals. This cluster resembled a pattern of retrogradely labeled DRN neurons after CTB injections into the third ventricle of the hamster (Leander et al., 1998), suggesting that the same DRN neuron might send axon collaterals to both the SC and to the ventricular system. However, a comparable configuration was not observed after fluorescent-tracer injections into the rat ventricular system (Simpson et al., 1998).

Neuronal populations within the DRN

The results of the present study provide evidence that neurons in the lateral DRN may be morphologically, anatomically, and neurochemically different from neurons in the medial DRN. At the rostral pole of the gerbil DRN, most 5-HT-ir neurons were located in the lateral populations. At all rostrocaudal levels, the lateral populations of the DRN contained a high proportion of SC-projecting neurons. In contrast, SC-projecting neurons were absent from the medial portion of the rostral DRN. Likewise, in the rat, most thalamic- and SC-projecting neurons also occur in the lateral wings of the DRN (Waterhouse et al., 1993). Gerbil neurons in the lateral DRN consistently showed higher 5-HT immunoreactivity and were conspicuously multipolar, compared with less intensely 5-HT-immunoreactive neurons in the medial DRN. Similar observations also have been reported in rabbit (Bjarkam et al., 1997) and in squirrel monkey (Charara and Parent, 1998). In the rostral DRN of the gerbil, 5-HT neurons in the lateral populations formed dorsal and ventral clusters (Figs. 2, 3). Similar clusters have been observed in the rabbit, with the dorsal cluster being designated as the "lateral DRN" and the ventral cluster as the "lateral extension of the ventromedial DRN" (Bjarkam et al., 1997). In gerbils, both of these clusters contain a comparable proportion of SC-projecting neurons; however, their anatomic segregation suggests that their projections to other visual targets (e.g., lateral geniculate complex, visual cortex) may be different. It appears that the lateral populations of 5-HT-ir neurons are continuous throughout the rostrocaudal extent of the DRN, because their morphology, 5-HT immunoreactivity, and the proportion of SC-projecting cells were comparable at all rostrocaudal levels. However, the dorsoventral location of the lateral cell populations changes, depending on the rostrocaudal level (Fig. 2).

The medial DRN in gerbils is a complex region that can be subdivided into several subpopulations. The present study has revealed a population of SC-projecting serotonergic neurons in the caudal interfascicular DRN. A some-

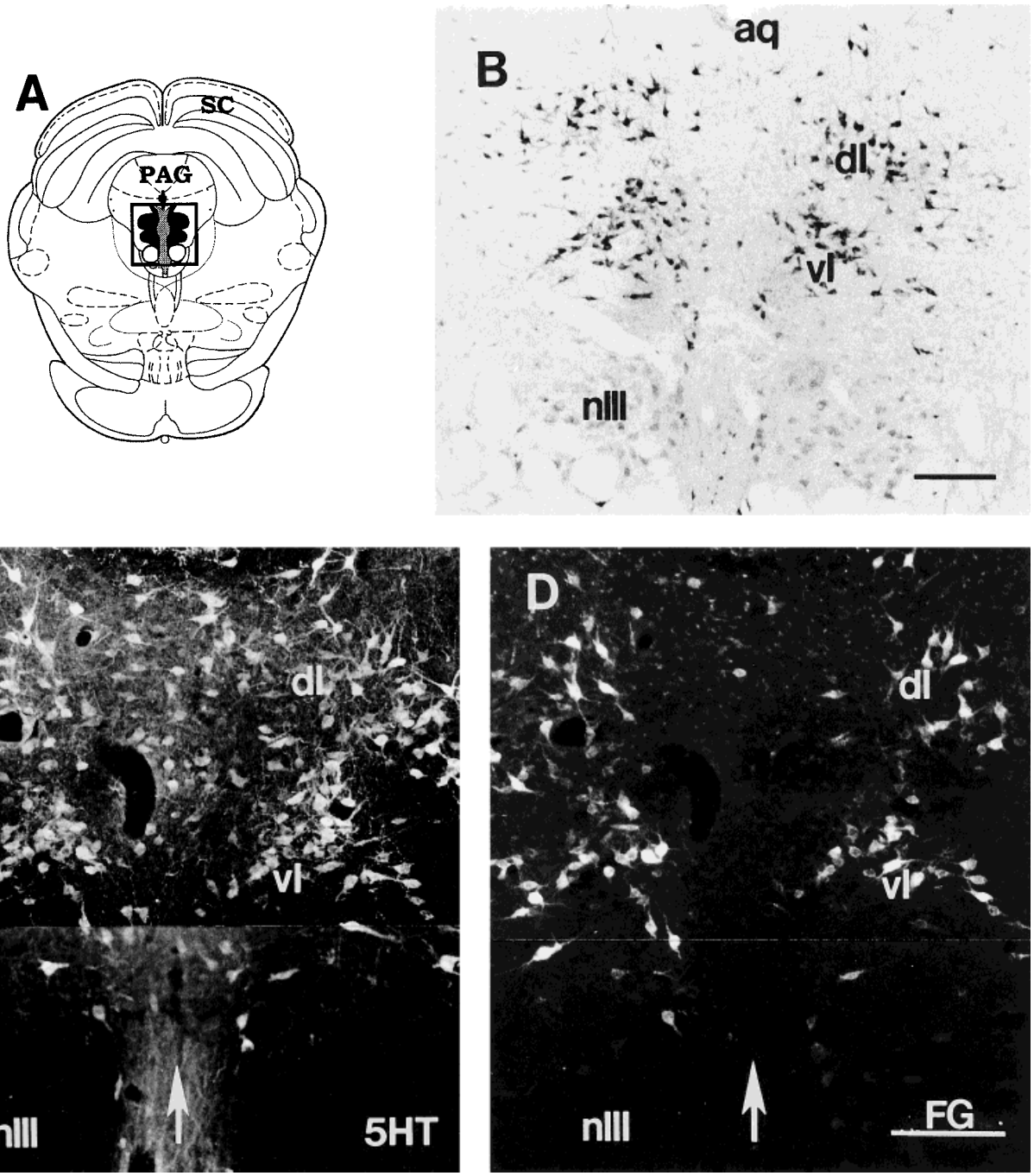

Fig. 3. Level 1: Distribution of 5-HT-immunoreactive (5-HT-ir) and retrogradely labeled cells in the dorsal raphe nucleus (DRN) after tracer injections into the superior colliculus (SC). Nearly all retrogradely labeled cells occur in the lateral DRN, forming dorsolateral (dl) and ventrolateral (vl) clusters. **A:** DRN subpopulations (as shown in Fig. 2) are superimposed on a schematic representation of the mesencephalon at the same level (from Paxinos and Watson, 1998). The square indicates the area shown in B, C, and D. **B:** Cholera toxin subunit-B (CTB)-labeled cells in the DRN after a bilateral CTB injection into the SC. **C,D:** Distribution of 5-HT-ir cells (in C) and FG-filled cells (in D) in the same DRN section after a bilateral FG injection into the SC. Arrows indicate the midline. PAG, periaqueductal gray; aq, aqueduct; nIII, oculomotor nucleus. Scale bars = 200 μm in B, 150 μm in D (applies to C,D).

what lower proportion of SC-projecting neurons exists in the ventromedial region that is located just dorsal to the interfascicular DRN (Fig. 2, Level 4). Interestingly, in rats, DRN neurons projecting to the visual cortex are clustered in the ventromedial/interfascicular region, but are confined, almost exclusively, to the rostral two-thirds of the DRN (Waterhouse et al., 1986, 1993). The population of rat DRN neurons projecting to the piriform cortex is restricted to the ventromedial part of the DRN as well (Datiche et al., 1995) and appears to include the interfascicular region.

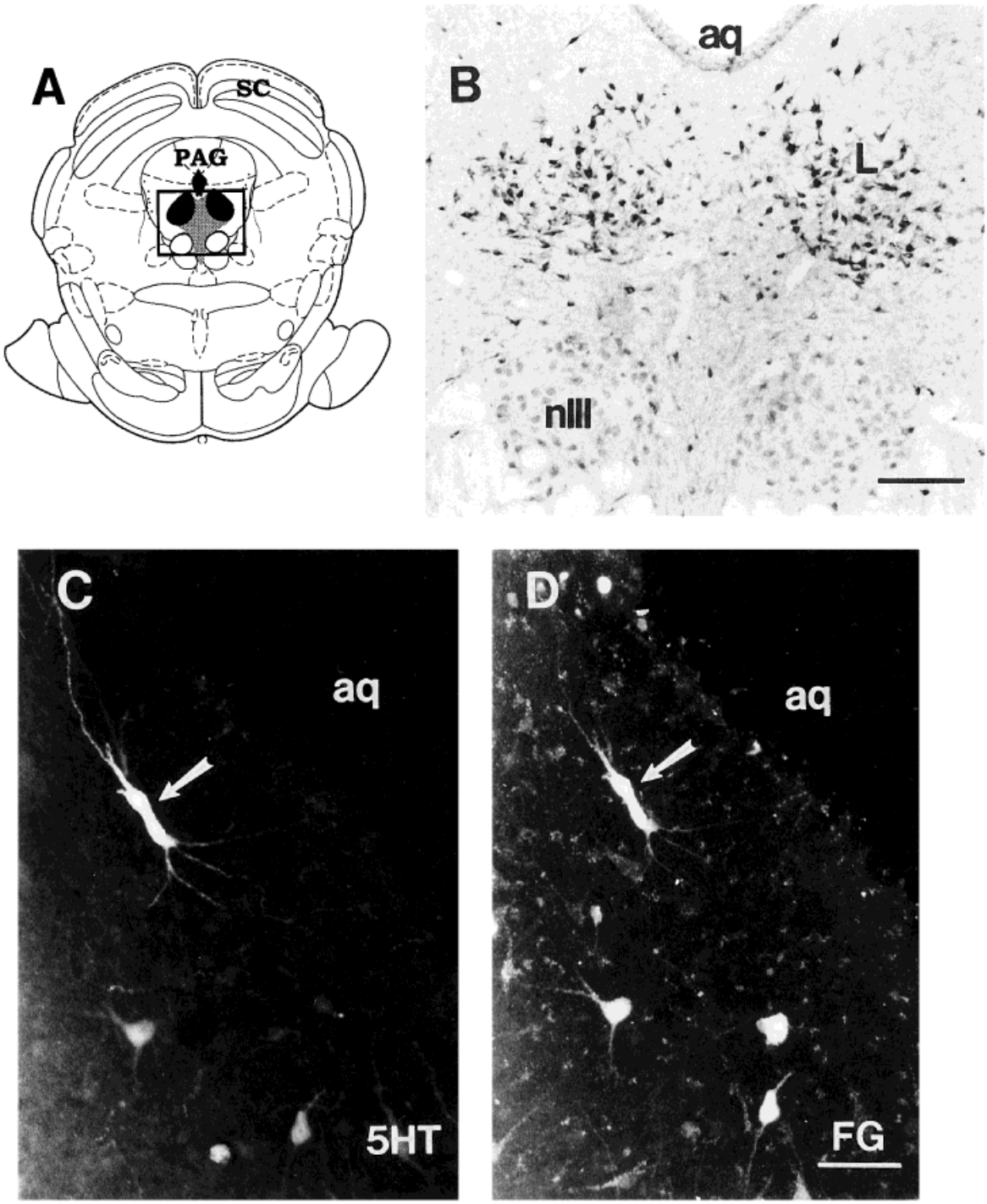

Fig. 4. Level 2: Distribution of 5-HT-immunoreactive (5-HT-ir) and retrogradely labeled cells in the dorsal raphe nucleus (DRN) after tracer injections into the superior colliculus (SC). Nearly all retrogradely labeled cells cluster in the lateral DRN (L). **A:** DRN subpopulations (as shown in Fig. 2) are superimposed on a schematic representation of the mesencephalon at the same level (from Paxinos and Watson, 1998). The rectangle indicates the area shown in B. **B:** Cholera toxin subunit-B (CTB) -labeled cells in the DRN after a bilateral CTB injection into the SC. **C,D:** 5-HT-ir cells (in C) and FG-filled cells (in D) in the lateral DRN (same section) after a bilateral FG injection into the SC. Note the large, double-labeled multipolar neuron (arrow). PAG, periaqueductal gray, aq, aqueduct; nIII, oculomotor nucleus. Scale bars = 200 μm in B, 50 μm in D (applies to C,D).

The caudal interfascicular/ventromedial DRN may be anatomically different from the rostral ventromedial DRN. In the present study, the term "interfascicular DRN" was used to designate the ventral cluster of DRN neurons isolated by the DTg at Level 4. More rostrally (anterior to the DTg), very few or no retrogradely labeled neurons were

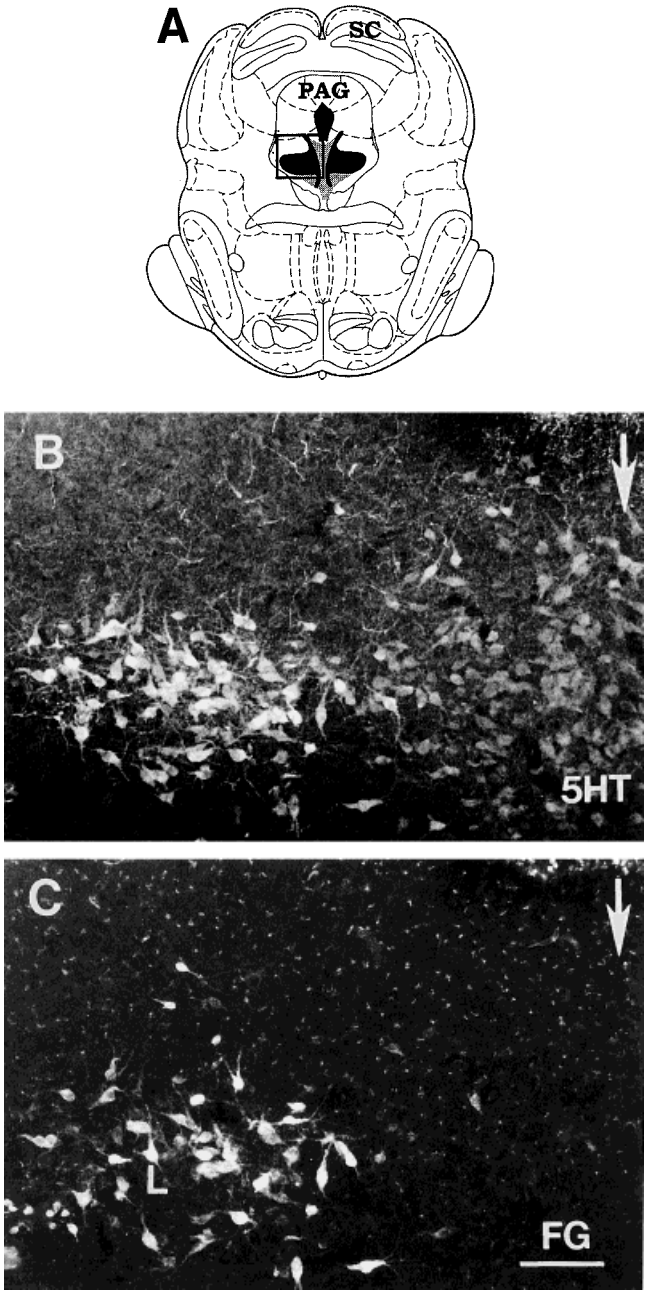

Fig. 5. Level 3: Distribution of 5-HT-immunoreactive (5-HT-ir) and retrogradely labeled cells in the dorsal raphe nucleus (DRN) after Fluoro-Gold (FG) injections into the superior colliculus (SC). Nearly all retrogradely labeled cells cluster in the lateral DRN (L); however, not all 5-HT-ir cells in the lateral DRN are also labeled with FG. **A:** DRN subpopulations (as shown in Fig. 2) are superimposed on a schematic representation of the mesencephalon at the same level (from Paxinos and Watson, 1998). The square indicates the area shown in B and C. **B,C:** Distribution of 5-HT-ir cells (in B) and FG-filled cells (in C) cells in the same DRN section after a bilateral FG injection into the SC. Only the left half of the DRN is shown; the right edge of each photograph represents the midline (arrow). Note that 5-HT-ir cells in the lateral DRN show higher immunoreactivity than 5-HT-ir cells in the medial DRN. PAG, periaqueductal gray. Scale bar = 100 μm in C (applies to B,C).

observed between the two MLF. Therefore, the term "interfascicular DRN" was not used to refer to regions anterior the rostral pole of the DTg. It appears that in gerbils and other species the interfascicular DRN at the level of the DTg may be a distinct population of neurons. For instance, in the squirrel monkey, SP-immunoreactive neurons occur almost in all subdivisions of the DRN rostrally but are confined to the area between the two MLF caudally (Charara and Parent, 1998). Recently, Leander et al. (1998) have shown that injections only in the caudal part of the DRN, at the level of the DTg, label efferent fibers in the deep pineal gland of the hamster. The interfascicular DRN also has been delineated in humans, although it has been described as extending to the rostral edge of the DRN (Baker et al., 1990).

Additional observations

Within the gerbil DTg, a very dense 5-HT-ir plexus was observed, which has not been described previously in other species. This plexus was a prominent landmark in the caudal DRN, where it divided the DRN into several anatomically distinct subpopulations. In rats, 5-HT-ir fibers in the DTg are much less prominent (unpublished observations); although, architectonically, the DTg appears to be similar in both rats and gerbils (Hyakawa and Zyo, 1983). Serotonergic neurons have been demonstrated in the cat and rat DTg (Takeuchi et al., 1982; Jacobs et al., 1984; Kitzman and Bishop, 1994), but were not observed in the gerbil DTg in the present study. Also, the extent of direct retinal afferents to the DRN is substantially different in the gerbil and rat DRN (Fite et al., 1998; unpublished observations). The gerbil DRN and its adjacent nuclei may have unique features that are associated with the well-developed visual system of this species.

The LDTg appears to be closely associated with the DRN and shows continuity with the lateral wings of the caudal DRN. At the interface of these two nuclei, populations of SC-projecting, 5-HT-ir neurons intermingle with SC-projecting, non–5-HT-ir neurons in the LDTg (Fig. 6A,B). Continuity also is suggested by studies on the neurochemical profiles of these cells in other species. For example, in the caudal DRN of the squirrel monkey, SP-, calretinin-, and parvalbumin-immunoreactive cells occur in continuity with similarly immunoreactive cells in the LDTg (Charara and Parent, 1998). Glutamate-immunoreactive neurons are interspersed among the cholinergic neurons in the rat LDTg and also occur in the DRN (Clements and Grant, 1990). According to Beitz et al. (1986), some neurons in the rat LDTg are 5-HT immunoreactive, which may be due to the inclusion of neurons at the margins of the lateral DRN.

Functional considerations

A growing body of evidence suggests that the raphe nuclei may have a complex internal organization. For example, neurons in the rat DRN may be electrically coupled. Stezhka and Lovick (1995) found that biocytin injections into DRN neurons resulted in dye-coupling of adjacent neurons in 48% of cases, and Richards et al. (1997) reported correlated activity of individual DRN neurons, which persisted after 5-HT depletion. Also, at the electron-microscopy level, a very complex synaptic organization has been described in the rat DRN (Wang et al., 1995, 1996, 1997, 1998). The DRN may contain the "complex synaptic arrangements" (CSAs), which consist of

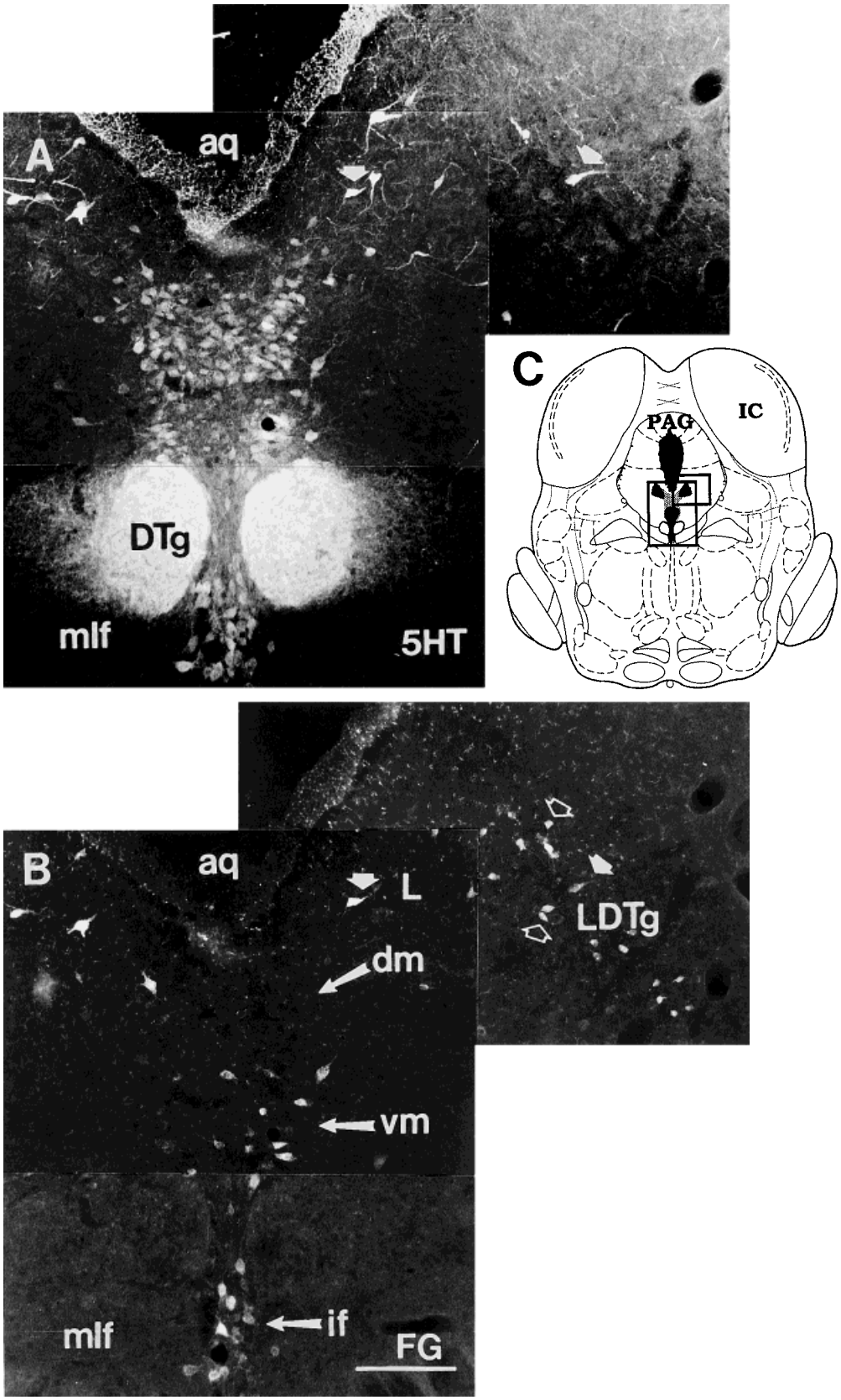

Fig. 6. Level 4. **A,B:** Distribution of 5-HT-immunoreactive (5-HT-ir) cells (in A) and Fluoro-Gold (FG) -filled cells (in B) in the same dorsal raphe nucleus (DRN) section after a bilateral FG injection into the superior colliculus. Note intense 5-HT-immunoreactive plexuses in the dorsal tegmental nuclei (DTg). Retrogradely labeled cells form clusters in the lateral (L), ventromedial (vm), and interfascicular (if) portions of the DRN, but retrogradely labeled cells are absent from the dorsomedial DRN (dm). Note that some double-labeled cells (small solid arrows) and cells labeled only with FG (open arrows) occur in both the lateral DRN and the laterodorsal tegmental nucleus (LDTg). **C:** DRN subpopulations (as shown in Fig. 2) are superimposed on a schematic representation of the mesencephalon at the same level (from Paxinos and Watson, 1998). Rectangles indicate the area shown in A and B. aq, aqueduct; mlf, medial longitudinal fasciculus; IC, inferior colliculus; PAG, periaqueductal gray. Scale bar = 150 μm in B (applies to A,B).

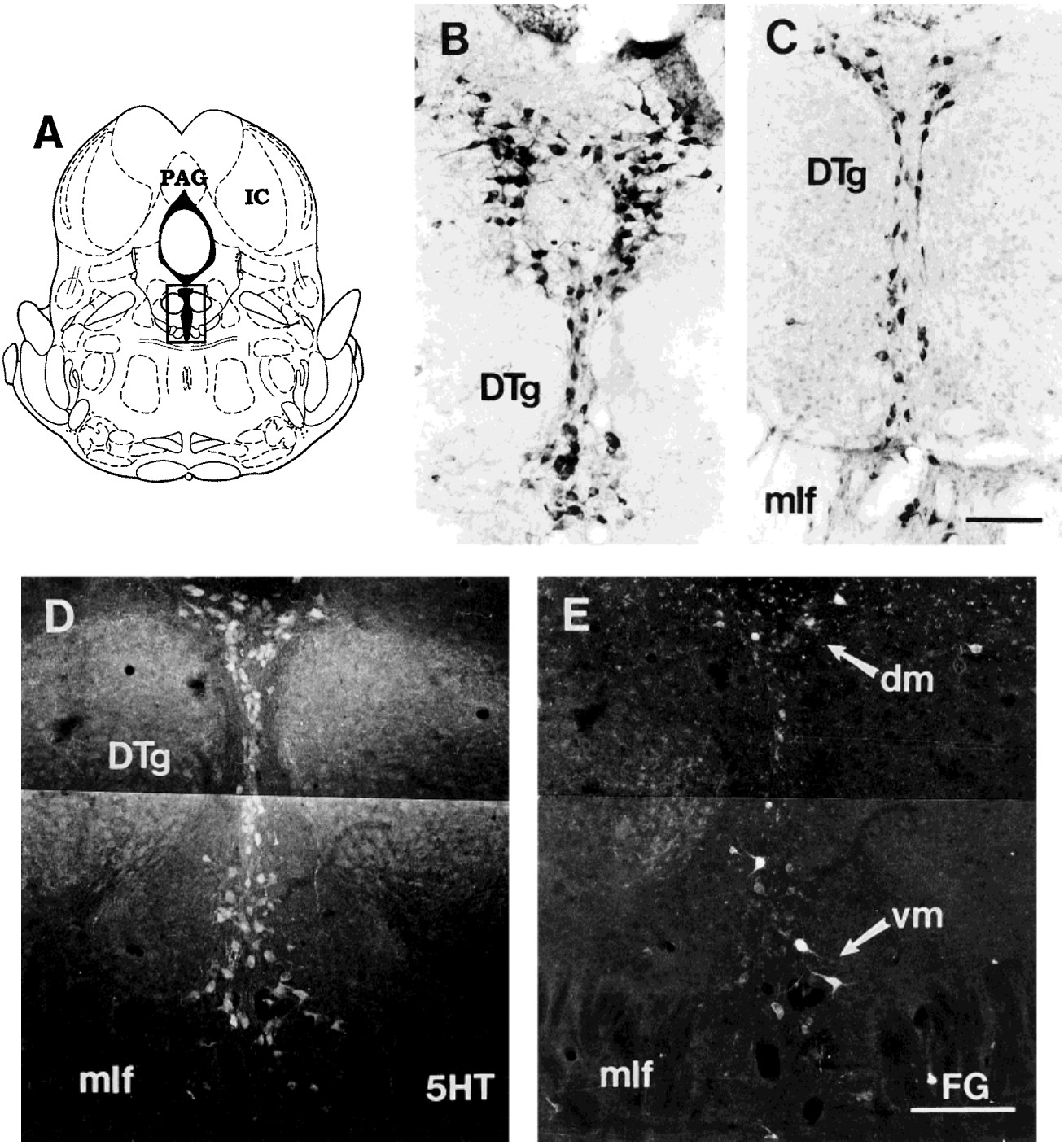

Fig. 7. Level 5: Distribution of 5-HT-immunoreactive (5-HT-ir) and retrogradely labeled cells in the dorsal raphe nucleus (DRN) after tracer injections into the superior colliculus (SC). **A:** DRN subpopulations (as shown in Fig. 2) are superimposed on a schematic representation of the mesencephalon at the same level (from Paxinos and Watson, 1998). The rectangle indicates the area shown in B, C, D, and E. **B,C:** Distribution of cholera toxin subunit-B (CTB) -labeled cells in the caudal DRN after a bilateral CTB injection into the SC: ring-like distribution of CTB-labeled cells at the border between Levels 4 and 5 (in B) and CTB-labeled cells in the middle of Level 5 (in C). **D,E:** Distribution of 5-HT-ir cells (in D) and Fluoro-Gold (FG) -filled cells (in E) in the same DRN section after a bilateral FG injection into the SC. Note 5-HT-ir plexuses in the dorsal tegmental nuclei (DTg) that separate the DRN into dorsomedial (dm) and ventromedial (vm) clusters. The dorsomedial DRN contains relatively few FG-filled cells, whereas the proportion of double-labeled cells is higher in the ventromedial DRN. PAG, periaqueductal gray; mlf, medial longitudinal fasciculus. IC, inferior colliculus. Scale bars = 100 μm in C (applies to B,C), 150 μm in E (applies to D,E).

circumscribed clusters of presynaptic and postsynaptic dendritic elements (Szentagothai, 1970). CSAs have been demonstrated in many brain nuclei and, in the DRN, may underlie the synchronization of neuronal activity, as described in the suprachiasmatic nucleus (Guldner and Wolff, 1996). In the DRN, some or all of these ultrastructural components may occur within the specific cell clusters that have been identified in the present study. The clustering observed at the light microscopy level may well be indicative of a considerable degree of interaction between neurons in a given cluster.

A functional differentiation of DRN neuronal clusters may occur at the level of 5-HT_{1A} inhibitory autoreceptors, which are abundant in the DRN (Wright et al., 1995). Although the distribution of 5-HT_{1A} receptors in the brain has been extensively studied (Wright et al., 1995; Pasqualetti et al., 1996; Childlow et al., 1998; Ito et al., 1999), little is known about how their distribution actually varies within the DRN. One binding study indicates that 5-HT_{1A} levels are highest in the ventral and interfascicular subpopulations of the human DRN, and that, within the interfascicular nucleus, 5-HT_{1A} receptor binding decreases in a rostrocaudal manner (Stockmeier et al., 1996). Even if serotonin levels were comparable throughout the DRN, neuronal clusters that express higher levels of the 5-HT_{1A} receptor would be more inhibited. Also, local variations of 5-HT levels may occur, which may be fine-tuned by somatodendritic release of 5-HT in the DRN (Adell et al., 1993).

At present, little information is available on the colocalization of two or more neurotransmitters/neuromodulators in DRN neurons with regard to their precise localization and their efferent connections. Also, little is known about how the neurochemical profiles of DRN neurons correlate with their electrophysiologic characteristics. DRN neurons exhibiting a regular firing pattern (1–5 spikes/s) are generally considered to be serotonergic (Aghajanian et al., 1968; Shima et al., 1986; Jacobs and Azmitia, 1992), and rapidly firing neurons with small somata are thought to be nonserotonergic (Park, 1987). In the rat, some DRN serotonergic neurons fire spikes in doublets or triplets (Hajos et al., 1995), and a population of DRN serotonergic neurons in the cat is strongly activated during oral-buccal movements and inhibited during orientation toward a novel stimulus (Fornal et al., 1996). It is possible that neurophysiologically identified classes of DRN neurons also may contain different complements of neurotransmitters/neuromodulators and may be localized in topographically different subdivisions of the DRN. For instance, the multipolar and intensely 5-HT-immunoreactive neurons located in the lateral subdivisions of the DRN (as observed in the present study) could represent a neurophysiologically distinct class.

In rodents, some interesting variations have been described in the serotonin system, some of which may be related to the differences in the visual system. For instance, 5-HT immunoreactive neurons have been found in the superficial layers of the superior colliculus in the hamster but not in the rat (Bennet-Clarke et al., 1991). Also, 5-HT–positive neurons have been observed in the suprachiasmatic nucleus of hamsters kept in constant darkness (Yamazaki et al., 1999). In the present study, very dense plexuses of serotonergic fibers were found in the dorsal tegmental nuclei of gerbils; however, a plexus of comparable 5-HT density does not seem to exist in rats (unpublished observations). Bhaskaran and Radha (1984) found that rats had the highest levels of 5-HT in the cortex during the light phase of the light/dark cycle; whereas Matsumoto et al. (1981) reported that gerbils showed the lowest levels of 5-HT in the cortex at light onset, and low 5-HT levels were maintained throughout the entire light phase. However, rats are nocturnal rodents, whereas Mongolian gerbils are crepuscular/diurnal, with peaks of activity occurring during the transitions between light and dark periods (Susic and Masirevic, 1986). The prominent clustering of SC-projecting neurons reported in this study could be related to the diurnality of the Mongolian gerbil and to the specific pattern of serotonin release at the efferent targets of the DRN. However, little information is available with regard to the underlying neural circuitry of the DRN, whereby photic stimulation may influence this major serotonergic nucleus and its widespread ascending pathways.

AKNOWLEDGEMENTS

We thank Ms. Lynn Bengston for her excellent technical assistance and Ms. Janice Cosentino for histologic assistance.

LITERATURE CITED

Adell A, Carceller A, Artigas F. 1993. In vivo brain dialysis study of the somatodendritic release of serotonin in the Raphe nuclei of the rat: effects of 8-hydroxy-2-(di-n-propylamino)tetralin. J Neurochem 60:1673–1681.

Aghajanian GK, Foote WE, Sheard MH. 1968. Lysergic acid diethylamide: sensitive neuronal units in the midbrain raphe. Science 161:706–708.

Angelucci A, Clasca F, Sur M. 1996. Anterograde axonal tracing with the subunit B of cholera toxin: a highly sensitive immunohistochemical protocol for revealing fine axonal morphology in adult and neonatal brains. J Neurosci Methods 65:101–112.

Baker KG, Halliday GM, Tork I. 1990. Cytoarchitecture of the human dorsal raphe nucleus. J Comp Neurol 301:147–161.

Beitz AJ, Clements JR, Mullett MA, Ecklund LJ. 1986. Differential origin of brainstem serotoninergic projections to the midbrain periaqueductal gray and superior colliculus of the rat. J Comp Neurol 250:498–509.

Bennet-Clarke CA, Mooney RD, Chiaia NL, Rhoades RW. 1991. Serotonin immunoreactive neurons are present in the superficial layers of the hamster's, but not the rat's, superior colliculus. Exp Brain Res 85:587–597.

Bhaskaran D, Radha E. 1984. Circadian variations in the monoamine levels and monoamine oxidase activity in different regions of the rat brain as a function of age. Exp Gerontol 19:153–170.

Bjarkam CR, Sorensen JC, Geneser FA. 1997. Distribution and morphology of serotonin-immunoreactive neurons in the brainstem of the New Zealand white rabbit. J Comp Neurol 380:507–519.

Cassel JC, Jeltsch H. 1995. Serotonergic modulation of cholinergic function in the central nervous system: cognitive implications. Neuroscience 69:1–41.

Chan-Palay V, Jonsson G, Palay SL. 1978. Serotonin and substance P coexist in neurons of the rat's central nervous system. Proc Natl Acad Sci USA 75:1582–1586.

Charara A, Parent A. 1998. Chemoarchitecture of the primate dorsal raphe nucleus. J Chem Neuroanat 72:111–127.

Chauvet N, Preto M, Alonso G. 1998. Tanycytes present in the adult rat mediobasal hypothalamus support the regeneration of monoaminergic axons. Exp Neurol 151:1–13.

Childlow G, Le Corre S, Osborne NN. 1998. Localization of 5-hydroxytryptamine1A and 5-hydroxytryptamine7 receptors in rabbit ocular and brain tissue. Neuroscience 87:675–689.

Clements JR, Grant SJ. 1990. Glutamate-like immunoreactivity in neurons of the laterodorsal tegmental and pedunculopontine nuclei in the rat. Neurosci Lett 120:70–73.

Cornwall J, Cooper JD, Philipson OT. 1990. Afferent and efferent connec-

tions of the laterodoral tegmental nucleus in the rat. Brain Res Bull 25:271–284.

Datiche F, Luppi P-H, Cattarelli M. 1995. Serotonergic and non-serotonergic projections from the raphe nuclei to the piriform cortex in the rat: a cholera toxin B subunit (CTb) and 5-HT immunohistochemical study. Brain Res 671:27–37.

Fite KV, Janusonis S, Foote W, Bengston L, Cosentino J. 1998. Retinal afferents in the Mongolian gerbil: innervation of structures outside the classical visual and visuomotor systems. Soc Neurosci Abstr 24:1394.

Fornal CA, Metzler CW, Marrosu F, Ribiero-do-Valle LE, Jacobs BL. 1996. A subgroup of dorsal raphe serotonergic neurons in the cat is strongly activated during oral-buccal movements. Brain Res 716:123–133.

Gonzalo-Ruiz A, Lieberman AR, Sanz-Anquela JM. 1995. Organization of serotoninergic projections from the raphe nuclei to the anterior thalamic nuclei in the rat: a combined retrograde tracing and 5-HT immunohistochemical study. J Chem Neuroanat 8:103–115.

Govardovskii VI, Rohlich P, Szel A, Khokhlova TV. 1992. Cones in the retina of the Mongolian gerbil, Meriones unguiculatus: an immunocytochemical and electrophysiological study. Vision Res 32:19–27.

Guldner FH, Wolff JR. 1996. Complex synaptic arrangements in the rat suprachiasmatic nucleus: a possible basis for the "Zeitgebber" and non-synaptic synchronization of neuronal activity. Cell Tissue Res 284:203–214.

Hajos M, Gartside SE, Villa AEP, Sharp T. 1995. Evidence for a repetitive burst firing pattern in a subpopulation of 5-hydroxytryptamine neurons in the dorsal and median raphe nuclei of the rat. Neuroscience 69:189–197.

Haring JH. 1991. Reorganization of the area dentata serotoninergic plexus after lesions of the median raphe nucleus. J Comp Neurol 306:576–584.

Harrington ME. 1997. The ventral lateral geniculate nucleus and the intergeniculate leaflet: interrelated structures in the visual and circadian systems. Neurosci Biobehav Rev 21:705–727.

Harvey JA. 1996. Serotonergic regulation of associative learning. Behav Brain Res 73:47–50.

Hyakawa T, Zyo K. 1983. Comparative cytoarchitectonic study of Gudden's tegmental nuclei in some mammals. J Comp Neurol 216:233–244.

Imai H, Steindler DA, Kitai ST. 1986. The organization of divergent axonal projections from the midbrain raphe nuclei in the rat. J Comp Neur 243:363–380.

Ito H, Halldin C, Farde L. 1999. Localization of 5-HT_{1A} receptors in the living human brain using [carbonyl-11C]WAY-100635: PET with automatic standardization technique. J Nucl Med 40:102–109.

Jacobs BL, Azmitia EC. 1992. Structure and function of the brain serotonin system. Physiol Rev 72:165–229.

Jacobs BL, Gannon PJ, Azmitia EC. 1984. Atlas of serotonergic cell bodies in the cat brainstem: an immunocytochemical analysis. Brain Res Bull 13:1–31.

Jacobs BL, Fornal CA. 1993. 5-HT and motor control: a hypothesis. TINS 16:346–352.

Jiang ZD, Moore DR, King AJ. 1997. Sources of subcortical projections to the superior colliculus. Brain Res 755:279–292.

King AJ, Jiang ZD, Moore DR. 1998. Auditory brainstem projections to the ferret superior colliculus: anatomical contribution to the neural coding of sound azimuth. J Comp Neurol 390:342–365.

Kitzman PH, Bishop GA. 1994. The origin of serotonergic afferents to the cat's cerebellar nuclei. J Comp Neurol 340:541–550.

Koh T, Nakazawa M, Kani K, Maeda T. 1991. Significant non-serotonergic raphe projection to the visual cortex of the rat An immunocytochemical study combined with retrograde tracing. J Hirnforsch 32:707–714.

Leak RK, Moore RY. 1997. Identification of retinal ganglion cells projecting to the lateral hypothalamic area of the rat. Brain Res 770:105–114.

Leander P, Vrang N, Moller M. 1998. Neuronal projections from the mesencephalic raphe nuclear complex to the suprachiasmatic nucleus and the deep pineal gland of the golden hamster (*Mesocricetus auratus*). J Comp Neurol 399:73–93.

Leger L, Charnay Y, Dubois PM, Jouvet M. 1986. Distribution of enkephalin-immunoreactive cell bodies in relation to serotonin-containing neurons in the raphe nuclei of the cat: immunohistochemical evidence for coexistence of enkephalins and serotonin in certain cells. Brain Res 362:63–73.

Matsumoto M, Kimura K, Fujisawa A, Uyama O, Yoneda S, Imaizumi M, Wada H, Abe H. 1981. Diurnal variations in monoamine contents in discrete brain regions of the mongolian gerbil (*Meriones unguiculatus*). J Neurochem 37. 3):792–794.

Meyer-Bernstein EL, Morin LP. 1996. Differential serotoninergic innervation of the suprachiasmatic nucleus and the intergeniculate leaflet and its role in circadian rhythm modulation. J Neurosci 16:2097–2111.

Mize RR, Horner LH. 1989. Origin, distribution, and morphology of serotonergic afferents to the cat superior colliculus: a light and electron microscope immunocytochemistry study. Exp Brain Res 75:83–98.

Moga MM, Moore RY. 1997. Organization of neural inputs to the suprachiasmatic nucleus in the rat. J Comp Neurol 389:508–534.

Moga MM, Saper CB. 1994. Neuropeptide-immunoreactive neurons projecting to the paraventricular hypothalamic nucleus in the rat. J Comp Neurol 346:137–150.

Montgomery S. 1995. Serotonin, sertraline and depression. J Psychopharmacol 9:179–184.

Park MR. 1987. Intracellular horseradish peroxidase labeling of rapidly firing dorsal raphe projection neurons. Brain Res 402:117–130.

Pasqualetti M, Nardi I, Lazinsky H, Marazziti D, Cassano GB. 1996. Comparative anatomical distribution of serotonin 1A, 1D alpha and 2A receptor mRNAs in human brain postmortem. Mol Brain Res 39:223–233.

Paxinos G, Watson C. 1998. The rat brain in stereotaxic coordinates, 4th ed. San Diego: Academic Press, Inc.

Petit J-M, Luppi P-H, Peyron C, Rampon C, Jouvet M. 1995. VIP-like immunoreactive projections from the dorsal raphe and caudal linear raphe nuclei to the bed nucleus of the stria terminalis demonstrated by a double immunohistochemical method in the rat. Neurosci Lett 193:77–80.

Pietrewicz AT, Hoff MP, Higgins SA. 1982. Activity rhythms in the Mongolian gerbil under natural light conditions. Physiol Behav 29:377–380.

Richards CD, Hajos M, Sharp T. 1997. Correlations in activity of 5-HT neurones within the dorsal raphe nucleus. Soc Neurosci Abstr 23:1228.

Shen H, Semba K. 1994. A direct retinal projection to the dorsal raphe nucleus in the rat. Brain Res 635:159–168.

Shima K, Nakahama H, Yamamoto M. 1986. Firing properties of two types of nucleus raphe dorsalis neurons during the sleep-waking cycle and their responses to sensory stimuli. Brain Res 399:317–326.

Shiromani PJ, Schwartz WJ. 1995. Towards a molecular biology of the circadian clock and sleep of mammals. Adv Neuroimmunol 5:217–230.

Simpson KL, Fisher TM, Waterhouse BD, Lin RC. 1998. Projection patterns from the raphe nuclear complex to the ependymal wall of the ventricular system in the rat. J Comp Neurol 399:61–72.

Stamp JA, Semba K. 1995. Extent of colocalization of serotonin and GABA in the neurons of the rat raphe nuclei. Brain Res 677:39–49.

Stezhka VV, Lovick TA. 1995. Dye coupling between dorsal raphe neurones. Exp Brain Res 105:383–390.

Stockmeier CA, Shapiro LA, Haycock JW, Thompson PA, Lowy MT. 1996. Quantitative subregional distribution of serotonin1A receptors and serotonin transporters in the human dorsal raphe. Brain Res 727:1–12.

Susic V, Masirevic G. 1986. Sleep patterns in the Mongolian gerbil, *Meriones unguiculatus*. Physiol Behav 37:257–261.

Szentagothai J. 1970. Glomerular synapses, complex synaptic arrangements, and their operational significance. In: Schmidt FO, editor. The neurosciences second study program. New York: Rockefeller University Press. p 427–443.

Takeuchi Y, Kimura H, Sano Y. 1982. Immunocytochemical demonstration of the distribution of serotonin neurons in the brainstem of the rat and cat. Cell Tissue Res 224:247–267.

Van Bockstaele EJ, Biswas A, Pickel VM. 1993. Topography of serotonin neurons in the dorsal raphe nucleus that send axon collaterals to the rat prefrontal cortex and nucleus accumbens. Brain Res 624:188–198.

Vertes RP. 1991. A PHA-L analysis of ascending projections of the dorsal raphe nucleus in the rat. J Comp Neurol 313:643–668.

Vertes RP, Fortin WJ, Crane AM. 1999. Projections of the median raphe nucleus in the rat. J Comp Neurol 407:555–582.

Villar MJ, Vitale ML, Hokfelt T, Verhofstad AAJ. 1988. Dorsal raphe serotoninergic branching neurons projecting both to the lateral geniculate body and superior colliculus: a combined retrograde tracing-immunocytochemical study in the rat. J Comp Neurol 277:126–140.

Wang Q-P, Guan J-L, Nakai Y. 1995. Distribution and synaptic relations of NOS neurons in the dorsal raphe nucleus: a comparison to 5-HT neurons. Brain Res Bull 37:177–187.

Wang Q-P, Guan J-L, Nakai Y. 1996. Electron microscopic study of GABAergic synaptic innervation of neurotensin-immunoreactive neurons in the dorsal raphe nucleus. Brain Res 730:118–124.

Wang Q-P, Guan J-L, Nakai Y. 1997. Electron microscopic study of

GABAergic synaptic innervation of nitric oxide synthase immunoreactive neurons in the dorsal raphe nucleus. Synapse 25:24–29.

Wang Q-P, Guan J-L, Ochiai H, Nakai Y. 1998. An electron microscopic observation of the vesicular transporter-immunoreactive fibers in the rat dorsal raphe nucleus. Brain Res Bull 46:555–561.

Waterhouse BD, Mihailoff GA, Baack JC, Woodward DJ. 1986. Topographic distribution of dorsal and median raphe neurons projecting to motor, sensorimotor, and visual cortical areas in the rat. J Comp Neurol 249:460–476.

Waterhouse BD, Border B, Wahl L, Mihailoff GA. 1993. Topographic organization of rat locus coeruleus and dorsal raphe nuclei: distribution of cells projecting to visual system structures. J Comp Neurol 336:345–361.

Wiklund L, Leger L, Persson M. 1981. Monamine cell distribution in the cat brain. A fluorescence histochemical study with quantification of indoloaminergic and locus coeruleus cell groups. J Comp Neurol 203:613–647.

Wright DE, Seroogy KB, Lundgren KH, Davis BM, Jennes L. 1995. Comparative localization of serotonin 1A, 1C, and 2 receptor subtype mRNA in rat brain. J Comp Neurol 351:357–373.

Yamazaki S, Alones V, Irelan M, Menaker M. 1999. Serotonin-containing cell bodies in novel brain locations: effects of light input. Neuroreport 10:431–435.